

ГЕОИНФОРМАЦИОННОЕ МОДЕЛИРОВАНИЕ, ВИРТУАЛЬНЫЕ ГЕОГРАФИЧЕСКИЕ СРЕДЫ И КОНЦЕПЦИЯ ЦИФРОВОЙ ЗЕМЛИ

GEOINFORMATION MODELING, VIRTUAL GEOGRAPHICAL ENVIRONMENTS AND THE CONCEPT OF DIGITAL EARTH

Jean A. Doumit¹

DOI: 10.24057/2414-9179-2018-2-24-241-249

EVALUATION OF MULTISCALE TERRAIN ROUGHNESS BASED ON UAV DATASETS: A CASE OF A LEBANESE REGION

ABSTRACT

Surface Roughness is an important geomorphological variable, no single definition exists; however, within the context of geomorphometry, we use surface roughness as an expression of variability in a topographic surface at a given scale.

The obtaining of a Digital Surface models (DSMs) at different scales and levels before the appearance of Unmanned Aerial Vehicles (UAV) was very rare or impossible. UAV's with advanced photogrammetry softwares which produce high-resolution Digital Surface Models. In this paper, we tested terrain roughness at multiscale DSM generated from six different UAV flight heights of 20, 40, 60, 120, 240 and 360 meters.

We tested an easily calculated terrain roughness index (TRI) and the vector roughness measure (VRM) which provides an objective quantitative measure of topographic heterogeneity.

TRI and VRM values of the six DSMs were correlated to understand the influence of spatial resolution on terrain heterogeneity, as a result of statistics and regression analysis the first three high-resolution DSMs save the degree of roughness and the last three generated from flight heights of 120, 240 and 360 meters lost the roughness degree with the loss of scale and spatial resolution.

KEYWORDS: UAV, DSM, Ruggedness.

INTRODUCTION

Surface roughness could be defined as a value ranging between smooth and complex surfaces, this paper specifically focuses upon the broad area at different scales of general geomorphology [Evans, 1729] and, more explicitly, on the quantification of surface-roughness variability using Digital Surface Models (DSMs) generated from UAV. Surface roughness is treated here as a geomorphometric variable influencing at the physiography of the terrain, not as a parameter due to the precision and accuracy of the generated digital surface models.

¹ Lebanese University, Faculty of literatures and human sciences, Beirut, Fanar, Lebanon, *e-mail*: jeandoumit@gmail.com

Measurement of terrain roughness is important for a number of disciplines of terrain quantifying characteristics have been evolving within fields such as geomorphology, engineering, biologists and ecologists [Doumit, 2017].

In terrains descriptions, roughness parameters should be established that can be used to describe surface irregularities and they should fulfill some requirements. The parameters should be descriptive and give the reader an image of the physical characteristics of the study area and should be easily measurable in the field so that large sites can be quickly sampled. If possible, roughness parameters should be selected that require similar types of field measurements with a minimal amount of equipment. Nowadays with the appearance of the Unmanned aerial vehicles and the advanced of Geographical Information Systems these parameters can be measured and compared at several different scales, and suitable for statistical and numerical analysis.

The simplest traditional method of terrain complexity is the profile method, by providing multi-sections on the terrain it is very easy to evaluate roughness of the terrain.

Hobson among the first scientists who calculated terrain Roughness using computer technologies, he wrote in Fortran language modules for calculating roughness parameters such as: comparison of the estimated actual surface area with the corresponding planar area; bump elevation frequency distribution; and the distribution of planes [Hobson, 1967].

With the fast evolution of GIS and geoinformatics methods, many scientists worked on the development of other methods for calculating terrain roughness such as: the application of Fourier analysis [Stone, Dugundji, 1965] geostatistics [Herzfeld et al., 2000], the fractal dimension of a surface [Elliot, 1989; Doumit, Pogorelov, 2017].

From the first recognized traditional methods for quantifying roughness was the land surface roughness index (LSRI) developed by [Beasom et al., 1983]. This index is a function of the total length of topographic contour lines in a given area.

[Riley et al., 1999] developed a terrain roughness index (TRI) that is derived digital elevation models (DEM) implemented in a geographical information system (GIS). TRI uses the sum of changes in elevation within an area as an index of terrain roughness.

Based on [Hobson, 1972] method developed for measuring surface roughness in geomorphology, a Vector Roughness Measure (VRM) quantifies terrain roughness by measuring the dispersion of vectors orthogonal to the terrain surface.

In this study we tested the regression between VRM and TRI values at the six different levels and we provided a correlation analysis between the raster datasets of VRM, and TRI, to examine their distributions within each scale, we generated scatterplots and calculated descriptive statistics (Min, Max, SD, skewness, kurtosis and r^2) to characterize terrain heterogeneity at different level.

MATERIALS AND METHODS

A mountainous region of 1700 m an average elevation above the sea level occupying an area of 2 hectares, Zaarour region on the western Lebanese mountainous chain characterized by a bare land without urbanizations and vegetation cover. The benefit of the study bare area is that Digital Surface Models are acting as Digital Terrain models, because of the empty area excluded from manmade activities and vegetation.

At big scale the micro-relief of the study area highlighting small terrain structure (ridges and valleys) due to small streams from snow melting processes, these structures are very narrow and gives the terrain a heterogeneity of textures and forms influenced by the scale changing.

Drones have been widely used as an apparatus for aerial photography, for many agricultural and terrain analysis applications, one of the advantages of UAV is the availability and fast photogrammetry mission execution at different altitudes.

An autopilot DJI Phantom 3 with a camera of 14 megapixels at a focal length of 3.61 mm flies the study area at different Heights. The flight paths of all missions were identical and designed in a mobile application called Litchi, the study area and the flight parameters (coordinates, height, time, etc...). All datasets (photos) of the six missions of different flight heights were processed in Agisoftphotoscan software for the extraction of Digital Surface Models (DSM). Before starting the aerial surveying, well-distinguishable 10 control points were evenly distributed within the area of interest for scaling and georeferencing the resulted data. Ground control points (GCP) were collected with Global Positioning System (GPS) in stereographic coordinate system.



Fig. 1. Google map background with the study area location of Zaarour region (Lebanon) figure from [Doumit, Pogorelov, 2016]

The drone took Aerial photography with 60 % overlapping and 50 % side lapping. SfM-based 3D methods operate on the overlapping images. The drone flight in an autonomous way, defined by waypoints to avoid image coverage gaps, every surface that will be reconstructed needs at the minimum to be covered by at least 2 images taken from different positions.

After executing the flight missions and data capturing, image processing was made in Agisoft Photoscan, following these steps: Control points establishment, Image capturing, Feature detection and image alignments, points cloud generation surface interpolation and Digital Surface Models generation.

The project constituted from field and office parts, the field works allowing us the installation and surveying of ground control points. The office part of data processing repeated 6 times englobing the above listed workflow steps, begins from key points detection ending by the generation of the six DSM's.

Fig. 1 shows six DSM of the study area of different spatial resolutions, FH-20 of 20 meters' flight height with a very high-resolution data set highlighting all the terrain details even rocks texture, passing by FH-60 the terrain is smoothed with some concave and convex areas and ending by FH-360 of 360 meters'.

These 6 DSM can be classified visually from fig. 2 by rough and smooth, FH-20, FH-40 and FH-60 for rough and FH-120, FH-240 and FH-360 for smooth, also figure 2 constitute an interval of scales and smoothness showing the generalization at different scales.

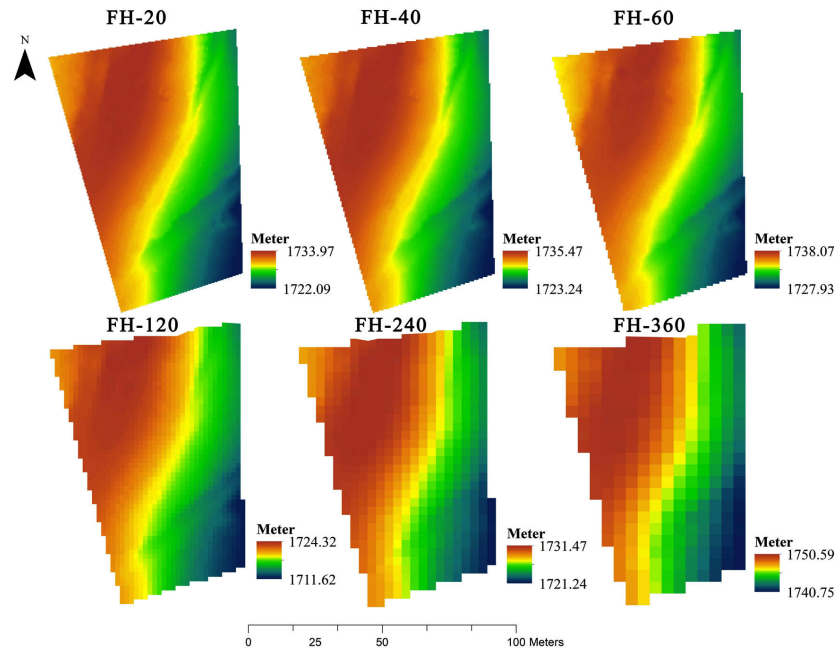


Fig. 2. Multiscale DSM obtained from image acquisition and processing

Table 1. Spatial resolutions of the six generated DSMs

DSM	Spatial resolution (m)
FH-20	0.4
FH-40	0.6
FH-60	0.80
FH-120	1.70
FH-240	3.20
FH-360	4.50

As per table one different flight altitude lead to different spatial resolution (pixel size), the higher spatial resolution of 0.40 m which showing all terrain details and textures, otherwise the lower spatial resolution of 4.50 m quite good for geomorphological analysis at a local scale.

Our study is independent from DSM accuracy and precision it will test roughness at six different levels expressed by flight height of a drone at 20, 40, 60, 120, 240 and 360 meters. The flight datum was calculated from the same takeoff points of the drone of the six flights.

As this study is restricted to evaluating array-based geomorphometric methods for calculating surface Roughness, an input DSM is required for further analysis. DSM selection criteria were based on spatial resolution, with a high-spatial-resolution DSM required in order to test the heterogeneity across a range of resolutions and within the study area presenting multiscale Roughness features.

The Terrain Roughness Index (TRI) based on an index described by [Riley et al., 1999] that calculated the sum change in elevation between a grid cell and its eight neighboring grid cells table 2 by squaring the eight differences in elevation, summing the squared differences, and taking the square root of the sum.

[Valentine et al., 2004] calculated the average of the absolute values of the eight differences in elevation, by using the TRI equation given as:

$$TRI = [abs\{grid(0,0) - grid(-1,-1)\} + abs\{grid(0,0) - grid(0,-1)\} + abs\{grid(0,0) - grid(1,-1)\} + abs\{grid(0,0) - grid(1,0)\} + abs\{grid(0,0) - grid(-1,1)\} + abs\{grid(0,0) - grid(0,1)\} + abs\{grid(0,0) - grid(-1,0)\} + abs\{grid(0,0) - grid(1,1)\}]/8 \quad (1)$$

Table 2. 3×3 grid of the TRI equation values

1, -1	0, -1	1, -1
-1, 0	0, 0	1, 0
-1, 1	0, 1	1, 1

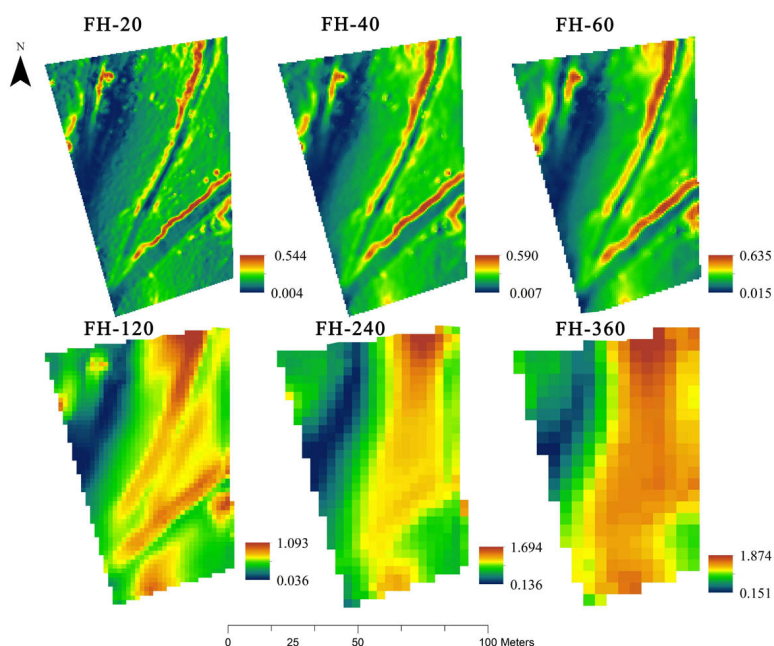


Fig. 3. TRI maps at different flight altitudes 20, 40, 60, 120, 240 and 360 above the datum

TRI high values at FH-20 shows details in ridges and water erosion traces, in FH-60 structures are very smoothed, FH-120 shows the pixel's boundaries and at FH-360 the map is totally pixelated. It is very clear in this map the disappearance of the small structures with the loss of spatial resolution, running from coarse to smooth then to pixelated surfaces.

Based on a method developed for measuring surface roughness in geomorphology [Hobson, 1972], the surface of elevation values can be divided into planar triangles very similar to Triangulated Irregular Network (TIN models) and normal to these planes represented by unit vectors. Values of vector mean strength (R), and dispersion (k) can be calculated for each square cell. In smooth areas, with similar elevations, the vector strength is expected to be high and the vector dispersion to be low since the vectors will become parallel fig. 4. In rough areas, the nonsystematic variation in elevation will result in low vector strength and high vector dispersion. The inverse of k can be a better representation of roughness [Mark, 1975].

Based on slope and aspect definitions, normal unit vectors of every grid cell of a digital elevation model (DEM) are decomposed into x, y and z components.

DSM resolution dependent from the flight height, in fig. 4 the topographic surface profile showing the terrain variation, at high spatial resolution vectors are very dense and orientated in several directions otherwise for low spatial DSM resolution as per example FH-360 vectors and far from each other perpendicular to segments expressing geometrical terrain forms.

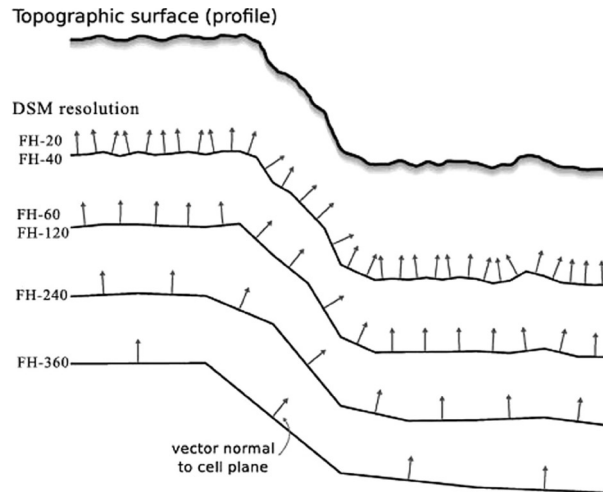


Fig. 4. Vector dispersion method used to calculate surface roughness at different scales for a topographical surface.
Graphic from [Grohmann et al., 2011]

The translation from the vector dispersion traditional method applied on topographic maps to Vector Roughness Measure (VRM) calculated by GIS algorithms, was done by applying the method and formulas used by [Veitinger et al., 2016]. Based on slope and aspect definition, the normal unit vector of every grid cell of a Digital Surface Model is decomposed into x, y, and z.

A resultant vector R is then obtained for every pixel by summing up the single components of the center pixel and its neighbors using a moving window technique.

$$R = \sqrt{(\sum x)^2 + (\sum y)^2 + (\sum z)^2} \quad (2)$$

The magnitude of the resultant vector is then normalized by the number of grid cell and subtracted from 1

$$VRM = 1 - \frac{R}{9} \quad (3)$$

where VRM is the vector ruggedness measure [Veitinger et al., 2016].

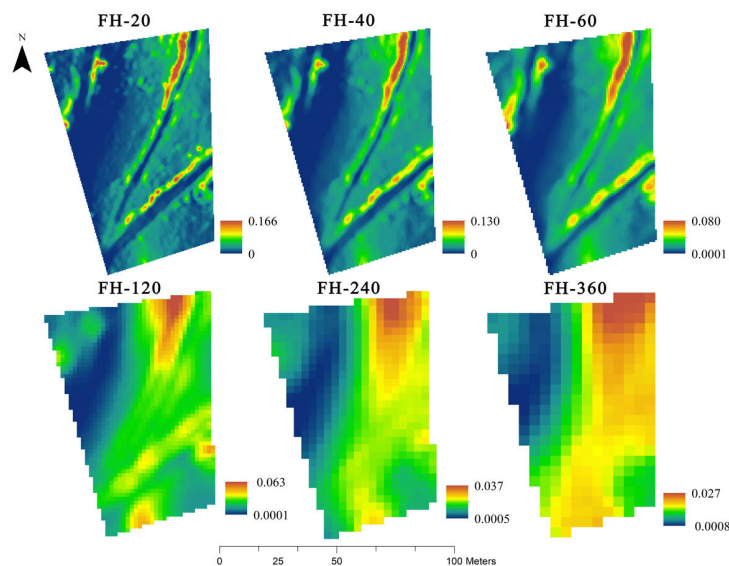


Fig. 5. VRM maps of the six DSMs

Fig. 5 shows the six VRM maps generated from DSM, by using formulae 3, for the first three high spatial resolution FH-20, FH-40 and FH-60, terrain structure are very fine highlighted similar to TRI map of fig. 3. The two indices TRI and VRM of the resulted roughness maps showed a loss in terrain heterogeneity and a trend to terrain homogeneity by a high degree of smoothness especially in the last three DSMs FH-120, FH-240, and FH-360. VRM measures the variation in terrain independent of its overall gradient, VRM is able to differentiate among terrain types.

RESULTS

In this work, we have tested two widely used methods: Terrain Roughness Index (TRI), Vector Roughness Measure (VRM), Terrain Roughness Index (TRI) calculates the sum change in elevation between a grid cell and its neighborhood, according to the algorithm by [Valentine et al., 2004].

Table 3. Terrain Ruggedness Index statistical values at each level. Std., standard deviation; Skew. Skewness; n, number of cell in a raster grid

	Mean	Std	Skew.	Kurtosis	n	Min.	Max.	Median	r ²
TRI-20	0.116	0.062	1.202	2.861	40436	0.005	0.544	0.112	0.0014
TRI-40	0.171	0.085	0.702	1.233	18522	0.008	0.591	0.172	0.00006
TRI-60	0.211	0.101	0.602	0.575	8891	0.016	0.636	0.208	0.0059
TRI-120	0.520	0.198	-0.424	-0.045	1901	0.037	1.093	0.552	0.0081
TRI-240	0.822	0.302	-0.385	-0.323	559	0.136	1.695	0.879	0.0033
TRI-360	1.113	0.381	-0.723	-0.448	286	0.152	1.874	1.234	0.0292

The statistics of the TRI values at each flight height listed in table 3, the values of Min., Max., Mean and Std. showed that the TRI values increased with the flight height hence with the scale. From the values of r² it is proven that no homogeneity of TRI values with their neighborhoods in each layer, it is normal especially for the high spatial resolution layer TRI-20, TRI-40, and TRI-60 with high n values.

For TRI-20 no symmetric data distribution because of the high skewness value of 1.202, but the evidence is that negative values for the skewness at TRI-120, TRI-240 and TRI-360 indicate data that are skewed left and positive values for the skewness indicate that high spatial resolutions layer TRI-20, TRI-40, and TRI-60 skewed right.

Table 4. Vector Ruggedness Measure statistical values at each level

	Mean	Std	Skew.	Kurtosis	n	Min.	Max.	Median	r ²
VRM-20	0.021	0.019	2.219	6.906	40436	0	0.166	0.017	0.013
VRM-40	0.021	0.017	1.753	4.757	18522	0	0.130	0.018	0.007
VRM-60	0.015	0.012	1.512	3.137	8891	0.0001	0.080	0.013	0.026
VRM-120	0.019	0.011	0.384	0.563	1901	0.0001	0.063	0.020	0.0001
VRM-240	0.015	0.008	0.119	-0.561	559	0.0006	0.037	0.015	0.0009
VRM-360	0.014	0.006	-0.289	-0.914	286	0.0009	0.027	0.015	0.0081

The distributions of roughness values (VRM) for the five levels were highly skewed to the right with the highest proportion of VRM values at the mean instead of FH-360 values skewed to the left.

Our results showed that TRI and VRM directly measured heterogeneity of terrain more independently of scale, and both indices exhibited a pattern of bias in that the minimum value of roughness increased with increasing spatial resolution.

A correlation analysis provided to understand the similarity between TRI and VRM.

High correlation recorder at all flight heights, the scattered plot of figure 6 shows a high degree of similarity in small values at FH-20, FH-40 and FH-60 expressed in the red elongated areas of figures 6, a, b and c.

At high flight height the concentration of the correlated values is moving from small to mean values with a trend to the right fig. 6, e, otherwise the correlation values of TRI and VRM in figure 6f became more scattered and less dense due to a dilution of similarity resulted from the changing of the spatial resolution (pixel size).

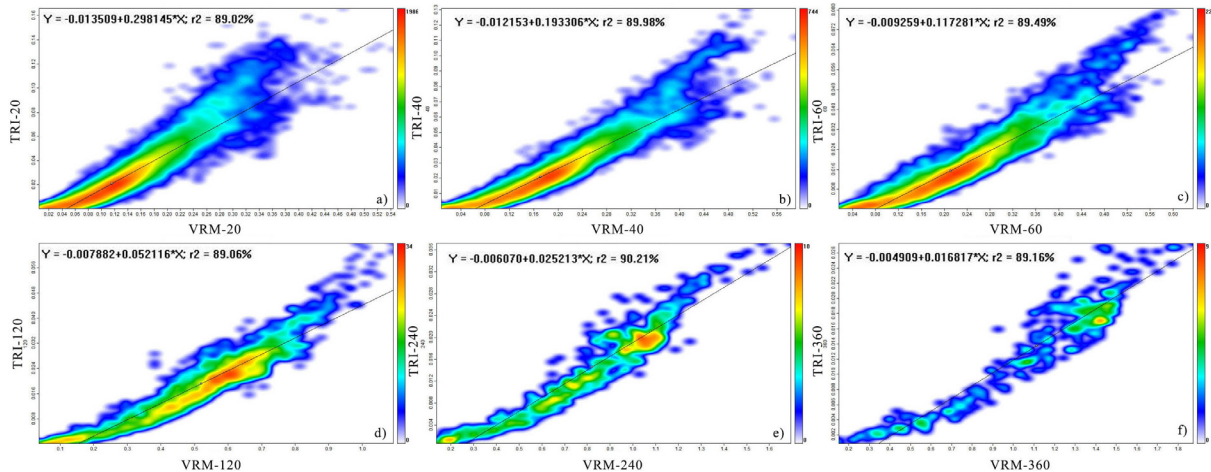


Fig. 6. Scatterplot of TRI and VRM ruggedness values at all levels of details:
a) FH-20, b) FH-40, c) FH-60, d) FH-120, e) FH-240, f) FH-360

We can say from figure 6 that the two roughness indices are very similar and have a high correlation and the degree of terrain roughness vary with the spatial resolution. Differences in the distributions of roughness, measured by VRM, and TRI reflected the characteristic terrain physiography of the terrain.

CONCLUSION

Surface Roughness in Earth sciences is used as an explanatory index. It is dependent upon exogenic and endogenic geographical processes. Many methods for surface Roughness measuring such as: area ratio, vector dispersion, the standard deviation of first and second terrain derivative (elevation, slope, and curvature) have been implemented in GIS and based on digital models.

The possibility of the production of digital models at different spatial resolution spatially UAV based one, allows fast and inexpensive multiscale analysis of surface Roughness. Two applied indices Topographic Roughness Index (TRI) and Vector Roughness Measure (VRM) at different scale level express a variety in terrain heterogeneity at a UAV flight height of 20, 40, 60, 120, 240 and 360.

Both indices show a roughness variation with scales and a transition from coarse to smooth between FH-60 and FH-120, a cartographic generalization influenced by flight height is very clear in figure 4 and 5. Our statistical and correlation analysis of roughness indices prove that multiscale and multilevel UAV flights datasets are: a visual cartographic generalization, a transition scale from level to another, a live roughness monitoring apparatus leads to a detection of fine scale/regional relief, and performance at a variety of scales.

Researchers must be aware of potential biases that originate in DSM at multiscale (different spatial resolution) when TRI and VRM values are interpreted. All DSMs contain inherent

inaccuracies due to the sources errors in original data. The elevation accuracy of a DSM is greatest in flat terrain and decreases in steep terrain where the roughness incises [Koeln et al., 1996]. Terrain roughness is a complicated geomorphometric parameter, it could be calculated in many ways, under many names roughness, micro relief, and others.

REFERENCES

1. *Beasom S. L., Wiggers E. P., Giordano R. J.* A technique for assessing land surface ruggedness. *Journal of Wildlife Management*. 1983. V. 47. P. 1163–1166.
2. *Doumit J. A., Pogorelov A. V.* Multi-scale Analysis of Digital Surface Models Based on UAV Datasets. *Modern Environmental Science and Engineering (ISSN 2333-2581)*, 2017. V. 3, No 7. P. 460–468.
3. *Elliot J. K.* An investigation of the change in surface roughness through time on the foreland of Austre Okstindbreen, North Norway. *Comput. Geosci.* 1989. V. 15, No 2. P. 209–217.
4. *Evans I. S.* General geomorphometry, derivatives of altitude, and descriptive statistics. *Spatial analysis in geomorphology* / R. J. Chorley, editor. New York: Harper and Row, 1972. P. 17–90.
5. *Grohmann C., Smith M., Riccomini C.* Multiscale analysis of topographic surface roughness in the Midland Valley, Scotland, *IEEE T. Geosci. Remote.* 2011. V. 49. P. 1200–1213.
6. *Herzfeld U. C., Mayer H., Feller W., Mimler M.* Geostatistical analysis of glacier-roughness data. *Ann. Glaciol.* 2000. V. 30, No 1. P. 235–242.
7. *Hobson R. D.* Surface roughness in topography: quantitative approach. *Spatial analysis in geomorphology*. New York: Harper and Row, 1972. P. 221–245.
8. *Koeln G. T., Cowardin L. M., Strong L. L.* *Geographical information systems* / T. A. Bookhout, ed. Research and management techniques for wildlife and habitats. Fifth ed., rev. The Wildlife Society, Bethesda MD. 1996. P. 540–566.
9. *Mark D. M.* Geomorphometric parameters: A review and evaluation, *Geografiska Annaler. Ser. A. Phys. Geography*. 1975. V. 57, No ¾. P. 165–177.
10. *Riley S. J., DeGloria S. D., Elliot R. A.* Terrain ruggedness index that quantifies topographic heterogeneity. *Intermountain journal of sciences*. 1999. V. 5, No 1–4.
11. *Stone R. O., Dugundji J.* A study of micro relief – Its mapping, classification and quantification by means of a Fourier analysis. *Eng. Geol.* 1965. V. 1, No 2. P. 89–187.
12. *Valentine P. C., Scully L. A., Fuller S. J.* Terrain Ruggedness Analysis and Distribution of Boulder Ridges and Bedrock Outcrops in the Stellwagen Bank National Marine Sanctuary Region – Posters presented at the Fifth International Symposium of the Geological and Biological Habitat Mapping Group, 2004, Galway, Ireland.
13. *Veitinger J., Purves R. S., Sovilla B.* Potential slab avalanche release area identification from estimated winter terrain: a multi-scale, fuzzy logic approach. *Natural Hazards and Earth System Sciences*. 2016. V. 16. P. 2211–2225.